Int. J. Electrochem. Sci., 14 **(2019)** 6267 – 6275, doi: 10.20964/2019.07.56

International Journal of ELECTROCHEMICAL SCIENCE
www.electrochemsci.org

Short Communication

One-step Growth of Well Aligned K-doped ZnO Nanotapers Using a Facile Electrochemical Route: Photocatalyst Application

Yang Ren[*], *Sen Han, Chen Liu, Yimin Feng, Kaoxue Li, Mingjun Song,*

College of Chemistry & Chemical and Environmental Engineering, Weifang University, Shandong 261061, China
[*]E-mail: renyangwf@163.com

Received: 6 March 2019 / *Accepted:* 2 May 2019 / *Published:* 10 June 2019

Large-scale oriented K-doped ZnO nanotapers were successfully grown on fluorine-doped tin oxide glass substrate using a facile electrochemical route. FESEM, TEM and HRTEM results indicate well-aligned taper-like single-crystalline ZnO hexagonal structure were achieved evidenced by a strong preferential growth along [0001] c-axis direction. Room temperature photoluminescence and Raman spectra results suggest the K doping introduced defect local electronic configuration. The K-doped ZnO nanotaper arrays used as photocatalysts present good photocatalytic performance to the degradation of 1,1,1-trichloro-2,2-bis (4-chlorophenyl) ethane (DDT) under simulated sunlight attribute to the K doping. The results reveal that taper-like K-doped ZnO nanostructures have significant and high photocatalytic actively and suitable alternative to other photocatalytic materials for environmental and water detoxification.

Keywords: K-doped ZnO nanotapers; Photocatalytic activities; Electrochemical method; Organochlorine pollutants

1. INTRODUCTION

Organochlorine pollutants are the widely used, toxic and most polluted types of Persistent Organic Pollutants (POPs) [1]. The photocatalytic oxidation technology by exploring semiconductor as photocatalyst is considered as promising environmental purification technologies due to their advantages of no secondary pollution and low cost [2]. In the past decades, zinc oxide (ZnO) nanostructures with various morphologies including nanoplates, nanorods, nanoneedles et al., have been widely considered for many applications, such as sensor, optical-devices and photocatalyst [3–5]. Among of current photocatalysts candidates, ZnO has high photocatalytic and quantum efficiency because of its effectiveness in the generation and separation of electron-hole pairs [6]. Besides, the taper-shape morphology creates larger active area than planar one, which increases the interfacial area contact. The

nanotaper is also an ideal shape for harvesting light due to the sides of the taper-like structure are tilted [7]. However, the optical absorption of ZnO production is restricted to UV light region of solar spectrum and limit its practical application. An important approach for its visible-light response is to find a method for the growth of P-type ZnO nanostructures, which is a complex and difficult task due to the large binding energy and the slow diffusion processes in the acceptor dopants [8-9]. Many attempts were made by various research groups to solve this issue through doping ZnO by different transition-metal ions for reducing the transition energy [10–14]. For instance, Cobalt (Co)-doped ZnO has been reported due to excess hyperchromic changes in the ZnO optical absorption, which is attributable to the band gap shrinkage. These changes by Co ions lead to a significant role in photocatalysis [13]. V-doped P-type semiconductor has been used for photooxidation of ethanol that revealed enhanced photo reactivity, but the side products were formic acid and carbon monoxide which are dangerous [14]. On the other hand, P-type ZnO can be achieved by doping with alkali metal elements and they are the most promising dopants materials as the shallow acceptors [15-16]. Although many reports on Na and Li-doped ZnO in improving the optical and electrical properties of ZnO have been published, very few researches have been reported for K-doped ZnO [16-20].

Motived by changing recombination trapping on the surface of photocatalysts and change the optical absorption to the visible light region, we herein proposed a facile electrochemical route to prepare the k-doped ZnO nanotapers which successfully control the process of crystallization. Furthermore, study on photocatalytic activities of K-doped ZnO were carried out under simulated solar light for photodegradation of 1,1,1-trichloro-2,2-bis (4-chlorophenyl) ethane (DDT) as modal organochlorine pollutant.

2. MATERIALS AND METHODS

All chemicals were of analytical grade and used without any treatment (Sinopharm Chemical Reagent Co., Ltd. , China). In a typical electrochemical deposition process, ZnO seed layer coated fluorine-doped tin oxide film was pre-fabricated via spin-coating method [21]. The precursor solution was prepared as follow. An equimolar mixture (0.1M) of hexamethylenetetramine (HMT) and zinc nitrate hexahydrate were first dissolved using DI water. Then, the solution was mixed with potassium nitrate (5 wt.%) as the precursor for K doping. After two hours stirring at room temperature, the pH of the solution was adjusted to 10 by adding few drops of NH_4OH. After another twenty minutes stirring, precursor solution was obtained. A computerized potentiostat instrument (model CHI660E) with a two-electrode system was employed to perform the growth of ZnO nanotapers onto FTO substrate (Figure 1). The electrochemical deposition cell contains 35 ml of above chemical solution. The solution was saturated with O_2 before deposition. The working electrode were fixed onto the substrate holder with effective area of 4 cm^2 and the distance to platinum counter electrode was kept at 3 cm. The chemical deposition constant current densities was of 0.5 mA/cm^2. The growth time was controlled for 1 hour and temperature was kept at 90 °C. After growing ZnO nanostructures, the obtained vertically aligned ZnO nanotaper structures on FTO (mass loading was 2.1 mg/cm^2) were washed using ethanol and dry at 120

^{o}C overnight. The undoped ZnO sample was prepared with similar procedure without the addition of potassium nitrate into precursor solution.

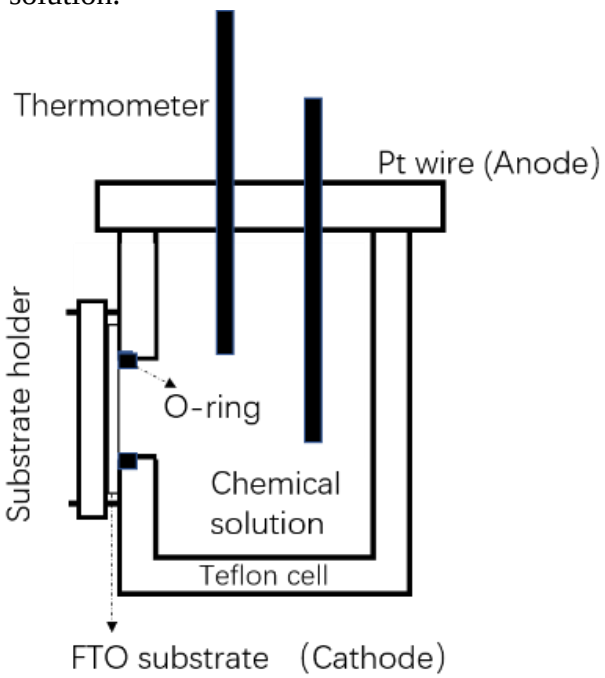

Figure 1. schematic diagram of electrochemical growth of K^+ doped ZnO nanotapers on FTO film.

The samples were characterized by FE scanning electron microscopy (FE-SEM, FEI Sirion 200) analysis. High-resolution transmission electron microscopy (HRTEM) (TECNAI G2 20S-TWIN, FEI) was employed to characterize size, morphology, and structure of the ZnO nanotapers. The optical properties were investigated by photoluminescence (PL) spectroscopy (LS55, PerkinElmer, CT, USA) and a LABRAM-HR Micro-Raman spectrometer (Jobin-Yvon) at room temperature.

The photocatalytic performance of K-doped ZnO nanotapers were assessed by the degradation of DDT (Aldrich) with a top irradiation reactor (50 ml) equipped with simulated sunlight resource (500-W Xe lamp with 340 nm cutoff filter). The catalyst loaded was controlled at 100 mg/L. The initial DDT aqueous concentration was of 20ppm. pH value was adjusted by drops of HCl or KOH (0.5M). Each concentration of DDT during the photodegradation with time were determined by GC-MS analysis (Thermo,TSQ8000 Evo)[22].

3. RESULTS AND DISCUSSION

Figure 2a shows High-magnified FESEM image of the K-doped ZnO nanotapers grown on the FTO substrate by electrochemical technique, which indicates K-doped ZnO crystals with taper-like structures and vertically aligned on a large scale. Each ZnO nanotaper contains of a hexagonal stalk with a tapering tip. As shown in figure 1b, the diameter of these nanotapers gradually reduces from bottom to top in the range of 160 ± 20 nm to 10 ± 5 nm, respectively, and with a length of around 2 μm. At an applied current density of 0.5 mA/cm^2, the polar planes have a tendency to disappear and only the faceted (1000) and (0101) habits finally appeared which had resulted in the tapering tips [23].

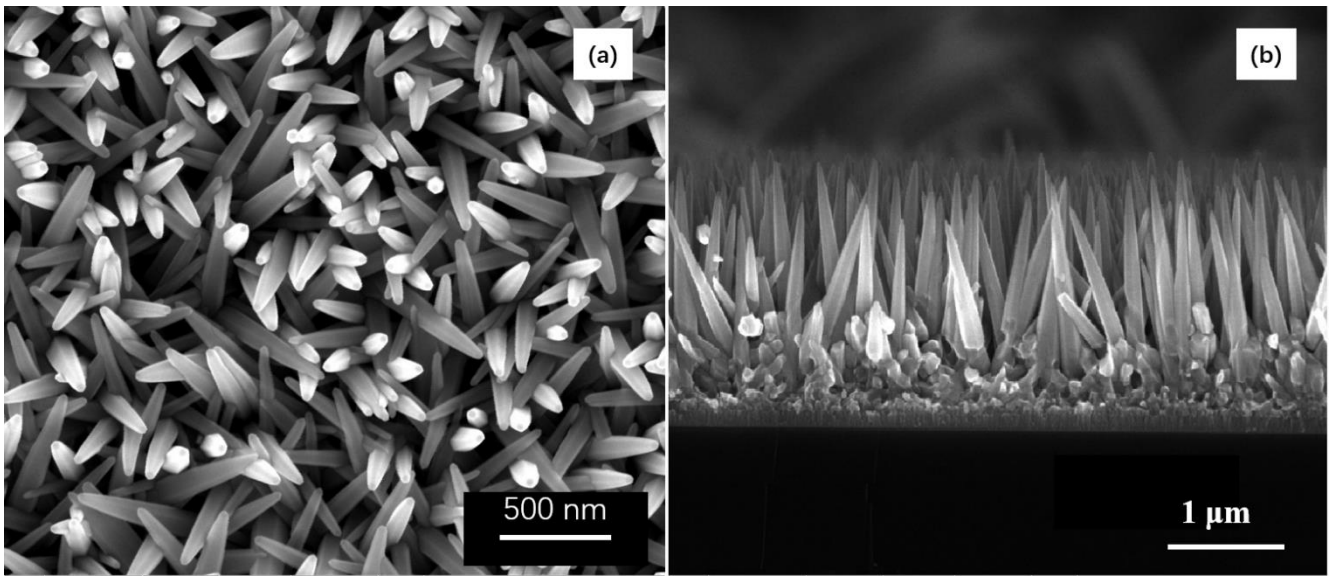

Figure 2. FESEM (a) Top view and (b) cross-sectional image of the K-doped ZnO nanotapers grown on FTO at current of 0.5 mA/cm^2 for 1 h at 90 °C

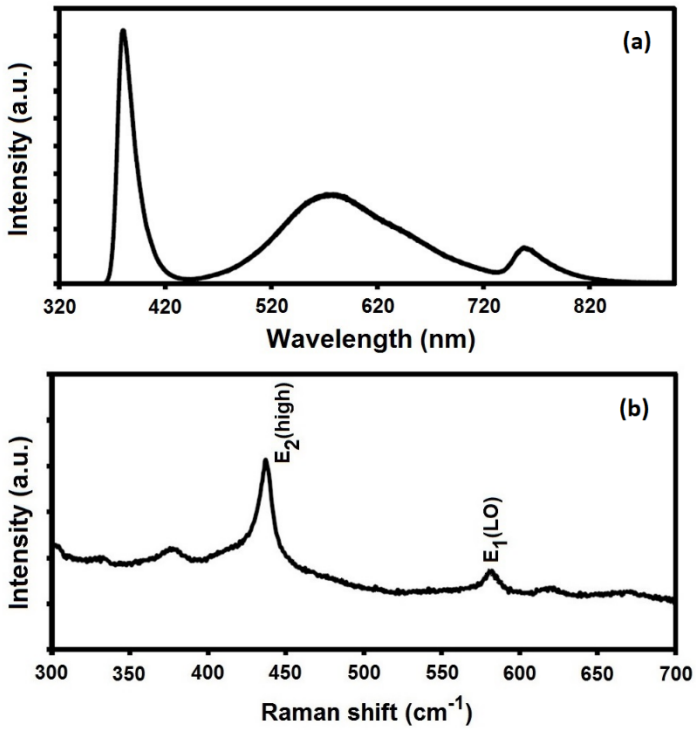

Figure 3. (a) PL spectra (λ_{ex} = 325 nm) and (b) Raman spectra of the K-doped ZnO nanotapers at room temperature (λ_{ex} = 514.5 nm).

Figure 3a shows the PL spectra of the K-doped ZnO nanotapers measured at room temperature. PL spectra of K-doped ZnO nanostructures show a strong ultraviolet (UV) emission peak appearing around 381 nm, and a weak visible emission peak at 576 nm. The broad visible band observed for ZnO nanostructures can be attributed to the deep level defects such as zinc interstitials and oxygen vacancies [24-25]. The narrow UV emission has been associated to the near band edge emission or radiative

annihilation of bound excitons [26]. Furthermore, the sharp UV emission suggests narrow distribution of the nanotapers, which has a good accordance with the FESEM results.

The backscattering Raman spectra for the K-doped ZnO nanotapers ranging from 300 to 700 cm^{-1} is presented in Figure 3b. The Raman spectra indicates a sharp and strong peak at 438 cm^{-1} corresponding to the $E_2^{(high)}$ mode which is related to a characteristic peak for the wurtzite hexagonal phase of ZnO [27]. A weak peak at 581 cm^{-1} related to $E_1^{(LO)}$ is shown for the K-doped ZnO nanotapers which can be associated with the formation of defects and impurities such as oxygen vacancy and zinc interstitial [28]. Therefore, it might be expected that the $E_1^{(LO)}$ mode is attributed to the defects introduced by K doping, which indicates a successful incorporation of K ions into the ZnO lattice.

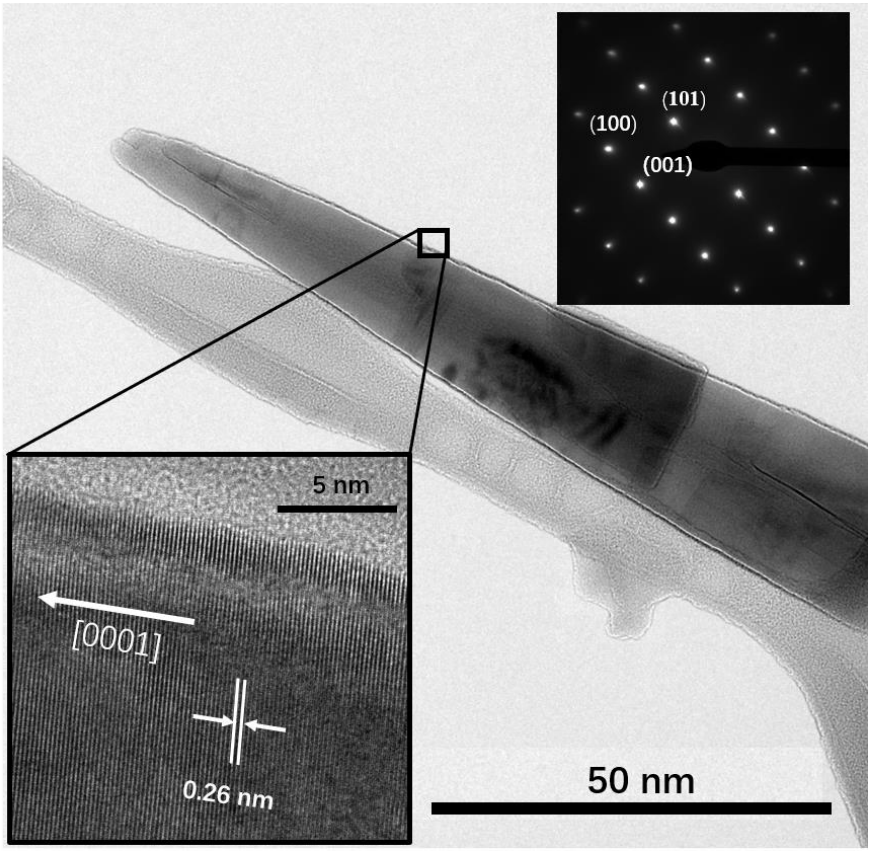

Figure 4. TEM image of the K-doped ZnO nanotapers. The insets show the HRTEM and SAED pattern.

Additional structural characterization of K-doped ZnO nanotapers was shown in Figure 4. A high magnification TEM image of an as-synthesized ZnO nanotaper reveals the full compatibility with the obtained FESEM results in terms of its morphology and dimensions. it is clearly observed from the HRTEM image (inset of Figure 4) that the lattice fringe spacing is approximately 0.26 nm which corresponds to the d-spacing of (002) crystal planes of the wurtzite hexagonal ZnO [29]. Combined with the select-area electron diffraction pattern (SAED) taken from the head of the nanotaper, it confirms that the nanotaper grows along the [0001] c-axis direction.

The solar light degradation experiment was performed on the DDT aqueous solution with different photocatalyst. Compared with undoped ZnO sample, the alkali metal ions doped in ZnO host

improve the photocatalytic activity as demonstrated in Figure 5a. The maximum degradation of 91% was attained by using K-doped ZnO catalyst under neutral pH condition within 4 hours. This evidently proves that ZnO doped with K^+ ions degrades DDT more effectively than undoped ZnO nanostructures. It can be associated to an increase in defect sites generated by K^+ doping which lead to an optical absorption enhancement in the visible region [30] K-doped ZnO generates electron–hole pair in the conduction and valence bands and the exciting electron from the conduction band of photocatalyst moves into the structure of DDT and mistunes its conjugated system that leads to the dechlorination of DDT [31-33].

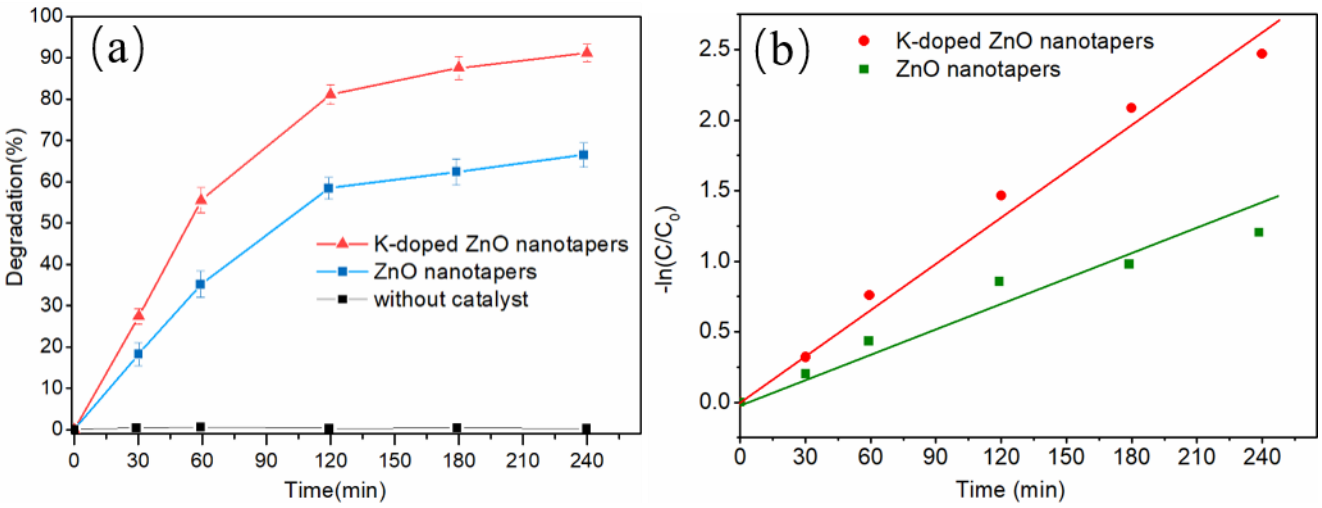

Figure 5. (a) Comparison of photocatalytic activity of K-doped ZnO and undoped ZnO nanotapers under simulated solar light. (20 ppm initiate DDT concentration and 100 mg/L catalyst loading at pH = 6.9) and (b) Plots of $-\ln(C/C_0)$ over irradiation time

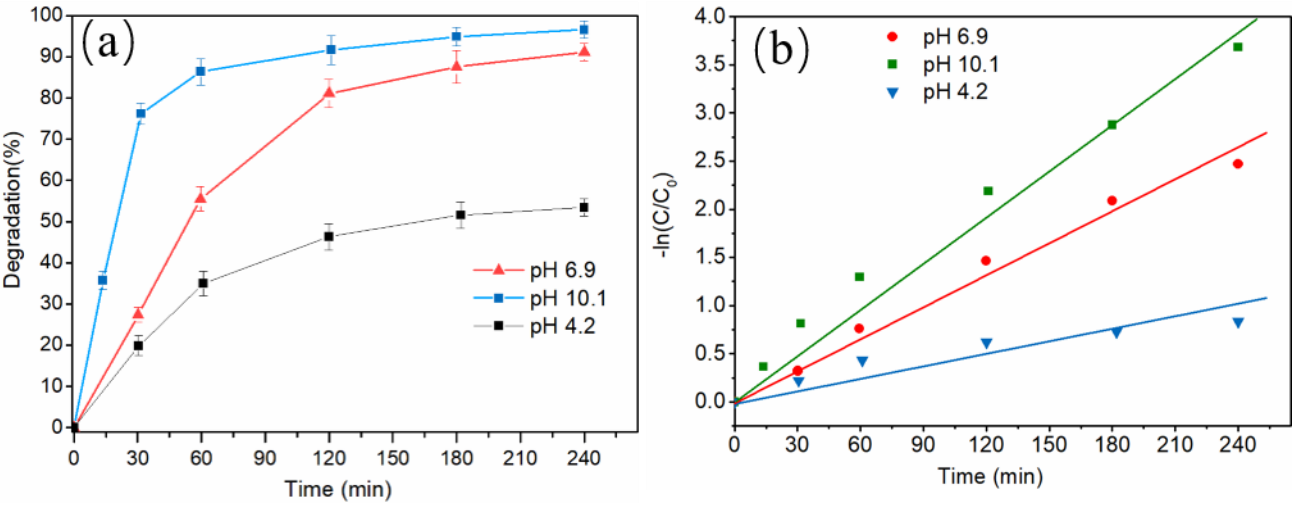

Figure 6. (a) Photocatalytic activity of K-doped ZnO nanotapers under different pH condition (20ppm DDT initiate concentration and 100 mg/L catalyst loading) and (b) Plots of $-\ln(C/C_0)$ over irradiation time

The Holes generate OH• (oxidation potential as high as 2.08 eV) at the valence band by reaction with OH^- or water can be used for ring-opening reactions until fully mineralized of aromatic hydrocarbon [31]. The photodegradation reaction kinetics of DDT (Figure 5b) followed the first-order [34] with the corresponding rate constants (k) of 0.0106 and 0.0051 min^{-1} for doped and undoped ZnO, respectively. It is clear that doping of taper-like ZnO with alkali metals such as K increases photocatalytic activities of ZnO nanostructures. The results reveal that ZnO doped with K^+ ions can be applied as a potential photocatalyst at visible light region.

Figure 6a indicates the photocatalytic activity of K-doped ZnO nanotapers under different pH condition. DDT photo-degradation rate with K-doped ZnO under pH = 10.4 is faster than pH = 6.9 and pH = 4.1. By taking constant DDT initiate concentration of 20 ppm, the maximum degradation efficiency of 97% was achieved under the pH=10.1. The corresponding rate constants (k) as revealed in Figure 6b are 0.0148 (pH =10.1), 0.0106 (pH =6.9), and 0.0032 min-1 (pH = 4.2) respectively. This phenomenon could attribute to the hole reacts with OH- in the photoreaction and concentration of generated OH• (hydroxyl radical) is high with an increasing pH [22]. The comparation of photocatalytic performance between some previously published report and the present study of similar catalysts for DDT removal application are summarized in table 1. The findings show that K-doped ZnO taper-like photocatalysis materials with low cost and high efficiency can be considered as one of the effective futuristic water purification methods.

Table 1. Comparison of proposed photocatalyst with other reported towards DDT degradation

Samples	Irradiation resource	Removal efficiency	Rate constant (min^{-1})	Ref.
P25 TiO_2/5 wt.% Pt	simulated sunlight (> 340 nm)	98 %	0.0093	[31]
Fe/TiO_2 film	UV radiation (365 nm)	95 %	0.0772	[22]
Heme-TiO_2 film	ultraviolet light (<370 nm)	60 %	--	[35]
ZnO nanorods	UV-Visible light (200–800 nm)	99 %	0.0061	[32]
N-doped TiO_2	UV / visible light	91% / 100 %	0.0121 / 0.1282	[36]
K-doped ZnO nanotapers film	Simulated Sunlight (340–800 nm)	97 %	0.0148	This work

4. CONCLUSIONS

K-doped ZnO nanotapers have been synthesized by low-cost and convenient electrochemical technique. The structural results exhibited the growth of taper-like ZnO single crystal along the [0001] direction. The Raman spectra indicated a successful incorporation of K ions into the ZnO lattice. Room temperature PL spectra showed sharp UV emissions centered at 381 nm and broad visible emissions in the range of 465 nm to 690 nm. The sharp feature appeared in the UV emission region suggests the narrow distribution of the nanotapers, which has a good accordance with the FESEM results. The results indicate that the photocatalytic activities of K-doped ZnO nanotapers are higher than undoped ZnO under simulated solar light. The development of doped ZnO photocatalysts might be considered an advance in

large-scale operation of heterogeneous photocatalysis by visible light response to address the issues of environmental pollution and water contamination.

ACKNOWLEDGEMENT
This work is financially supported by Shandong Province Natural Science Foundation (Grant No.ZR2018QEM003), Science and Technology Development Program of Weifang City (Grant No.20121311) and Doctoral Foundation of Weifang University (Grant No.2012BS12).

References

1. R. Ameta, S. Benjamin, A. Ameta, and S. C. Ameta, *Mater. Sci. Forum*, 734 (2012) 247.
2. K. M. Lee, C. W. Lai, K. S. Ngai, and J. C. Juan, *Water Res.*, 88 (2016) 428.
3. J. Rouhi, C. R. Ooi, S. Mahmud, and M. R. Mahmood, *Mater. Lett.*, 147 (2015) 34.
4. M. Husairi, J. Rouhi, K. Alvin, Z. Atikah, M. Rusop, and S. Abdullah, *Semicond. Sci. Technol.*, 29 (2014) 075015.
5. H. Oh, J. Park, W. Choi, H. Kim, Y. Tchoe, A. Agrawal, and G.-C. Yi, *Small*, 14 (2018) 1800240.
6. F. Zhang, W. Zhang, X. Luo, G. Feng, and L. Zhao, *Int. J. Electrochem. Sci.*, (2017) 3756.
7. T. Majumder, S. Dhar, P. Chakraborty, K. Debnath, and S. P. Mondal, *J. Electroanal. Chem.*, 813 (2018) 92.
8. S.-D. Baek, P. Biswas, J.-W. Kim, Y. C. Kim, T. I. Lee, and J.-M. Myoung, *ACS Appl. Mater. Interfaces*, 8 (2016) 13018.
9. S. U. Awan, Z. Mehmood, S. Hussain, S. A. Shah, N. Ahmad, M. Rafique, M. Aftab, and T. A. Abbas, *Phys. E Low-Dimens. Syst. Nanostructures*, 103 (2018) 110.
10. N. Sobana and M. Swaminathan, *Sep. Purif. Technol.*, 56 (2007) 101.
11. A. Sapkota, A. J. Anceno, S. Baruah, O. V. Shipin, and J. Dutta, *Nanotechnology*, 22 (2011) 215703.
12. N. V. Kaneva, D. T. Dimitrov, and C. D. Dushkin, *Appl. Surf. Sci.*, 257 (2011) 8113.
13. Z. Pezeshki-Nejad, S. Alikhanzadeh-Arani, A. E. Rezaee, and M. A. Kashi, *Ceram. Int.*, 45 (2019) 6912.
14. S. Klosek and D. Raftery, *J. Phys. Chem. B*, 105 (2001) 2815.
15. S. Tosoni, C. Di Valentin, and G. Pacchioni, *J. Phys. Chem. C*, 118 (2014) 3000.
16. Y. Wang, J. Piao, G. Xing, Y. Lu, Z. Ao, N. Bao, J. Ding, S. Li, and J. Yi, *J. Mater. Chem. C*, 3 (2015) 11953.
17. V. Bornand, *Thin Solid Films*, 574 (2015) 152.
18. N. Shakti and P. S. Gupta, *Mater. Today Proc.*, 5 (2018) 10149.
19. D. Akcan, A. Gungor, and L. Arda, *J. Mol. Struct.*, 1161 (2018) 299.
20. C.-L. Hsu, B.-Y. Jhang, C. Kao, and T.-J. Hsueh, *Sens. Actuators B Chem.*, 274 (2018) 565.
21. Q. Zhou, J. Wen, P. Zhao, and W. Anderson, *Nanomaterials*, 7 (2017) 9.
22. S.-J. Jang, M.-S. Kim, and B.-W. Kim, *Water Res.*, 39 (2005) 2178.
23. J. Rouhi, M. Alimanesh, S. Mahmud, R. A. Dalvand, C. R. Ooi, and M. Rusop, *Mater. Lett.*, 125 (2014) 147.
24. J. Rouhi, M. Alimanesh, R. Dalvand, C. R. Ooi, S. Mahmud, and M. R. Mahmood, *Ceram. Int.*, 40 (2014) 11193.
25. F. D. Ruiz-Ocampo, J. M. Zapien-Rodriguez, O. Burgara-Montero, E. A. Escoto-Sotelo, F. A. Nunez-Perez, and J. C. Ballesteros-Pacheco, *Int. J. Electrochem. Sci.*, 12 (2017) 4898.
26. F. S. Husairi, J. Rouhi, K. A. Eswar, A. Z. Zainurul, M. Rusop, and S. Abdullah, *Appl. Phys. A*, 116 (2014) 2119.
27. G. Vijayaprasath, R. Murugan, Y. Hayakawa, and G. Ravi, *J. Lumin.*, 178 (2016) 375.

28. C. Kumari, A. Pandey, and A. Dixit, *J. Alloys Compd.*, 735 (2018) 2318.
29. L. Wang, K. Xiong, Y. He, X. Huang, J. Xia, X. Li, Y. Gu, H. Cheng, and X. Meng, *CrystEngComm*, 19 (2017) 2294.
30. J. Wang, Z. Wang, B. Huang, Y. Ma, Y. Liu, X. Qin, X. Zhang, and Y. Dai, *ACS Appl. Mater. Interfaces*, 4 (2012) 4024.
31. R. Borello, C. Minero, E. Pramauro, E. Pelizzetti, N. Serpone, and H. Hidaka, *Environ. Toxicol. Chem.*, 8 (1989) 997.
32. G. Meenakshi and A. Sivasamy, *Ecotoxicol. Environ. Saf.*, 135 (2017) 243.
33. A. Alhadhrami, A. S. Almalki, A. M. A. Adam, and M. S. Refat, *Int. J. Electrochem. Sci.*, 13 (2018) 6503.
34. A. Zaleska, J. Hupka, M. Wiergowski, and M. Biziuk, *J. Photochem. Photobiol. Chem.*, 135 (2000) 213.
35. J. R. Stromberg, J. D. Wnuk, R. A. F. Pinlac, and G. J. Meyer, *Nano Lett.*, 6 (2006) 1284.
36. J. Ananpattarachai and P. Kajitvichyanukul, *J. Environ. Sci. Health Part B*, 50 (2015) 247.